Design and modeling of a D–shaped PCF refractive index sensor based on SPR effect

Amin Sayyad Tondro
Islamic Azad University of Fasa
mojtaba sadeghi (mojtaba.sadeghi.fasa@gmail.com)
Islamic Azad University Shiraz
Abbas Kamaly
Islamic Azad University of Fasa
Zahra Adelpour
Islamic Azad University Shiraz
Seyyed Ali Emamghorashi
Islamic Azad University of Fasa

Research Article

Keywords: Photonic crystal fiber, SPR, Sensor, refractive index, Sensitivity

Posted Date: April 21st, 2022

DOI: https://doi.org/10.21203/rs.3.rs-1332587/v1

Design and modeling of a D–shaped PCF refractive index sensor based on SPR effect

Amin Sayyad Tondro[1], Mojtaba Sadeghi[2,*], Abbas Kamaly[1], Zahra Adelpour[2], Seyyed Ali Emamghorashi[1]

[1]Department of Electrical Engineering, Fasa Branch, Islamic Azad University, Fasa, Iran

[2]Department of Electrical Engineering, Shiraz Branch, Islamic Azad University, Shiraz, Iran

Abstract

In this article, we propose and study a D–shaped plasmonic refractive index (RI) sensor. The numerical simulation is performed by the finite–element method (FEM). Results indicate that the proposed RI sensor is particularly proper for sensing in the wavelength range of 0.5 to 0.7 μm. When the analyte RI varies from 1.33 to 1.36, the highest wavelength sensitivity of 9500 nm/RIU and RI resolution of 6.5×10^{-6} RIU are obtained. Besides, the highest amplitude sensitivity of 215 RIU^{-1} is achieved with a high linearity of 0.99862. These results confirm the capability of the proposed sensor for rapid and accurate detection of RI change in biological and industrial applications.

Keywords: Photonic crystal fiber, SPR, Sensor, refractive index, Sensitivity.

1. Introduction

SPR sensors are very efficient in many sensing applications owing to their privilege sensitivity and simple functionality. Photonic crystal fiber (PCF) can be regarded as an adequate sensing base mainly due to its small dimension and flexibility that provide more premier sensing features unveiled by combination of the surface–plasmon–resonance (SPR) phenomenon [1, 2]. Referring to the structural characteristics of a PCF used to manage light

* Corresponding Author. Email: Sadeghi@shiraziau.ac.ir

transmission, a series of optical parameters including nonlinearity, dispersion, effective mode field area, and mode birefringence, can be engineered practically. Consequently, sensing performance can also become much better. In recent years, D–shaped PCF sensors have been growingly developed and considered owing to the SPR effect. A D–shaped SPR sensor based on an all–solid PCF was introduced by Tian et al. and showed at least 7300 nm/RIU for spectral sensitivity [3]. In another attempt, a D–shaped PCF–SPR sensor with average sensitivity of 7700 nm/RIU and resolution of 1.30×10^{-5} RIU was proposed for RI range of 1.43–1.46 [4]. Wu and coworkers suggested a novel D–shaped sensor with the sensitivity of 31000 nm/RIU in NIR region [5].

Focusing on the visible and NIR region of spectrum, we modeled and simulated a simple D–shaped PCF–SPR sensor and surveyed the structural characteristics that influence the pertinent sensitivity. Regarding the chemical stability and resonance output energy of excitation materials, we considered silver (Ag) as the sensing–layer medium. The effect of the structural parameters on the sensing performance of the modeled sensor was analyzed by the FEM, and investigated the sensing performance to the analyte RI variations.

2. Details of modeling

Fig.1a shows the cross–section illustration of the proposed sensor. The lattice pitch is Λ=4 μm, the diameter of air holes are represented by d_1 and d_2, respectively, and we set d_1 = 3.2 μm and d_2= 1.6 μm. The thickness of Ag layer (T_{Ag}) is set 40 nm. The background material of the designed PCF is fused silica. The FEM is employed to study the PCF–SPR properties and sensing performance. The FEM discretized mesh is shown in Fig. 1b. The RI of fused silica is given by Sellmeier equation [6]:

$$n(\lambda)=\sqrt{\varepsilon+\frac{A}{\lambda^2}+\frac{B\lambda_1^2}{\lambda^2-\lambda_1^2}} \qquad (1)$$

where λ exhibits a free space wavelength, and ε = 11.6858, λ_1 = 1.1071 μm, A = 0.939816 μm^2, and B = 8.10461×10^{-3}. The dielectric parameters of Ag can be determined from the L4 model [7]

$$\varepsilon(\omega) = \varepsilon_\infty + \frac{\sigma/\varepsilon_0}{i\omega} + \sum_{p=1}^{4} \frac{C_p}{\omega^2 + A_p\omega + B_p} \tag{2}$$

all constants of Eq. 2 were adopted from Ref [7].

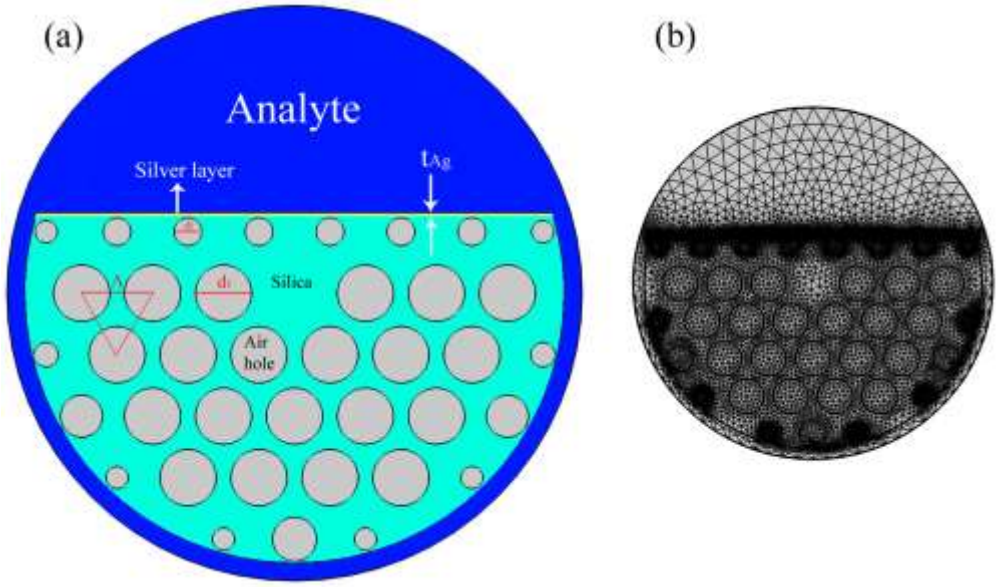

Fig.1. (a) cross–section view of the proposed sensor and (b) FEM discretized mesh.

The modes will couple, when their effective refractive index (n_{eff}) are equal. To investigate the coupling properties of the designed sensor, we display the n_{eff} curve and E– field distributions along with the loss spectra of the pertinent modes in Fig. 2. The confinement loss of the sensor can be characterized by using the following formula [7]

$$\alpha_{Loss}(dB/cm) = 8.686 \times \left(\frac{2\pi}{\lambda}\right) \times \mathrm{Im}(n_{eff}) \times 10^4 \tag{3}$$

The sensitivity of the sensor of the RI unit (RIU) can be defined as [8]

$$S_n\left(\mu m / RIU\right) = \frac{\Delta\lambda_{peak}}{\Delta n_{Anl.}} \tag{4}$$

where $\Delta\lambda_{peak}$ denotes the shift of the resonance peak.

Since no spectral manipulation is required, it is more cost effective to utilize the amplitude interrogation technique (AIT) to investigate the performance of the sensor. The amplitude sensitivity can be calculated by [9]

$$S_{Amp.}\left(RIU^{-1}\right) = -\frac{1}{\alpha\left(\lambda, n_{Anl.}\right)} \times \frac{\Delta\alpha\left(\lambda, n_{Anl.}\right)}{\Delta n_{Anl.}} \tag{5}$$

where α, $\Delta\alpha$ and $\Delta n_{Anl.}$ stand for loss, loss difference and variation of the analyte RI, respectively.

3. Results and Discussion

In the simulated structure, (a) x–polarization core fundamental mode (FM) (Fig. 2a), (b) y–polarization core FM (Fig. 2b), and (c) SPP mode in the sensing layer (Fig. 2c) are analyzed. When light interacts with Ag layer on the Ag–analyte interface, both x and y–polarization FMs appear in the core, but only x–polarization FM can stimulate the surface plasmons.

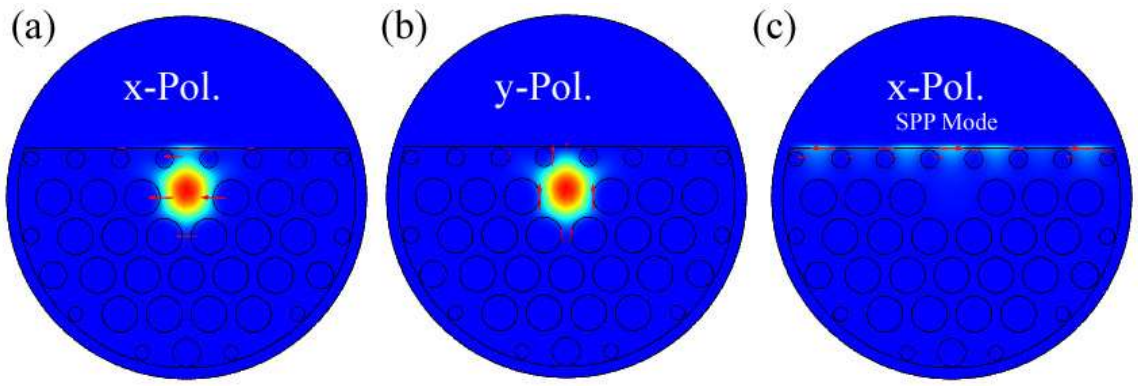

Fig. 2. Mode pattern of (a) x–polarization core (b) y–polarization core and (c) SPP fundamental mode.

Based on the dispersion relations of the x–polarization FM and plasmonic mode in Fig. 3, a detectable loss signal at the intersection (phase matching point) of the two RI curves is quite evident. At the mode–resonance conditions, the evanescent field in the fiber is remarkably boosted, and a strong loss peak rises. In our study, only x–polarization FM can resonate with SPP mode at λ= 500 nm. Therefore, only one loss peak at the intersection of the two curves rises that is very proper to be utilized in the sensing field. Owing to the uniqueness of resonance peak in the sensor, the accurate detection of the analyte RI can be gained.

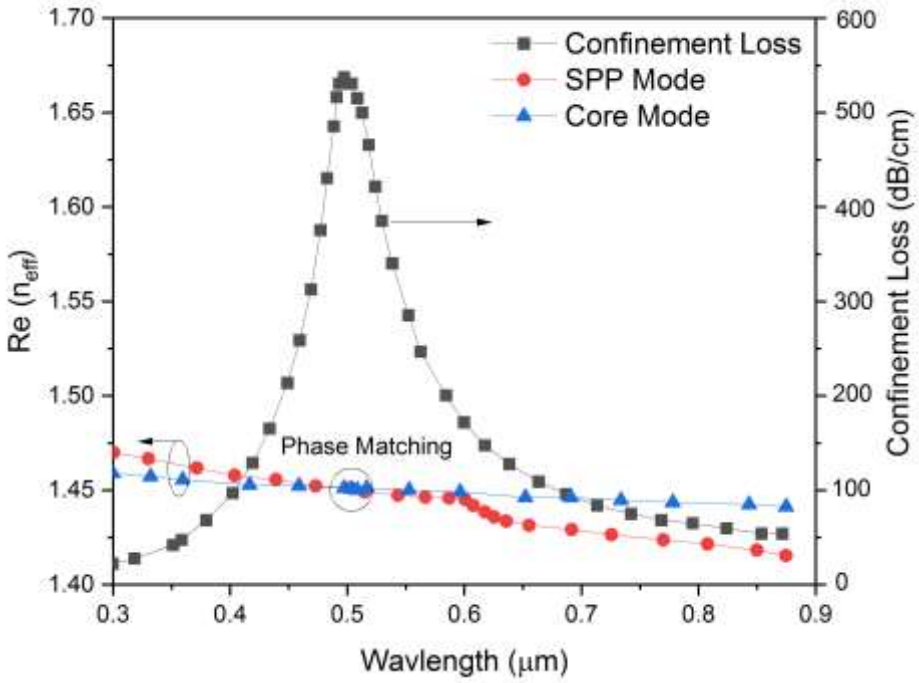

Fig. 3. The relation of radiation between the fundamental core–guided mode and SPP mode with $n_{Anl.}$=1.33.

The effect of the PCF structural parameters on the sensing characteristics of the proposed sensor is also investigated. Fig. 4 illustrates the loss spectra for different d_1 values with n_{Anl} =1.33. As it is obvious, the position of resonance peak is red–shifted as d_1 increases. At the same time, the intensity of resonance signal also changes; particularly in the case of d_1= 4.2μm, the sharpness of the signal is reduced and widened. This coincides with decrement in

the core area which made it difficult to keep good single–mode transmission of the PCF, so x–polarization FM cannot produce a strong mode–coupling effect with the SPP mode.

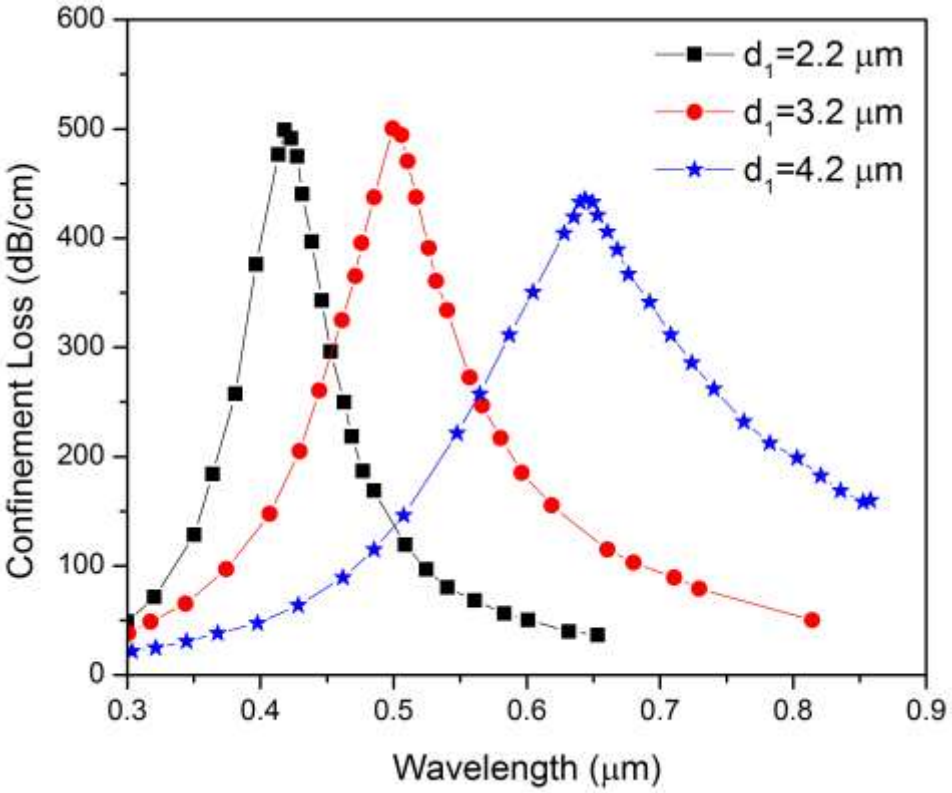

Fig. 4. Variation of the confinement loss spectra for different d_1 values.

For d_1= 2.2 and 3.2 μm, the energy generated by the latter is also slightly larger than that of the former; if more loss energy is generated, the peak will be easier to detect, hence the case of d_1= 3.2 μm is opted for the next step of analysis.

The effect of different silver–layer thicknesses (T_{Ag}) on the sensor performance is also studied and shown in Fig.5. As the T_{Ag} increases, the confinement loss is was blue–shifted, and the pertinent intensity decreases. That is why the thinner thickness of the silver layer causes more light–matter interaction that leads to more free oscillation of surface plasmon. This event also boosts the evanescent field near the dielectric interface. Hence, T_{Ag}=20 nm is selected as the optimum thickness for the next stage of simulation.

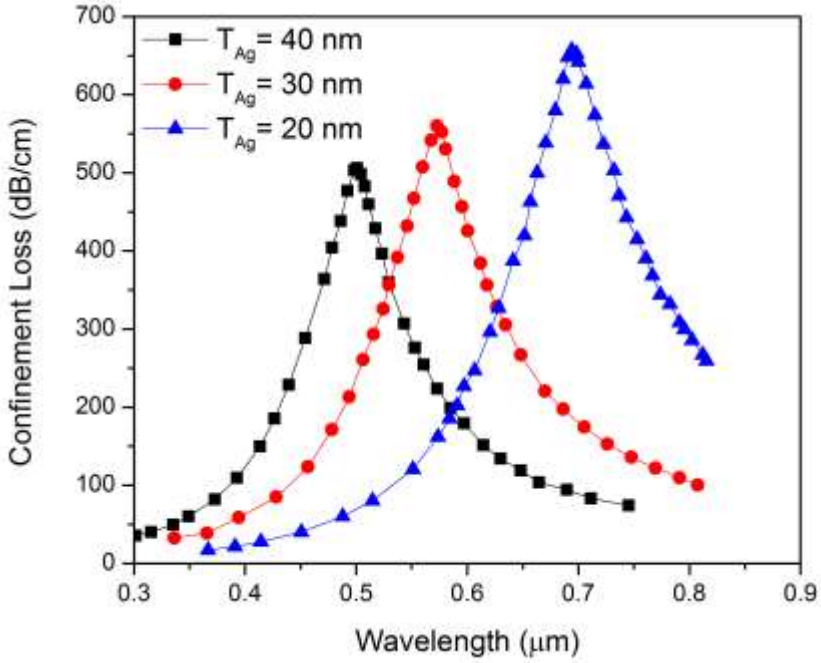

Fig. 5. Variation of the core mode confinement loss spectra of the proposed RI sensor for different thickness of silver layer.

The influence of different lengths of the lattice pitch on the confinement loss spectra of the proposed RI sensor is also investigated. Fig. 6 depicts the calculated confinement loss spectra for three different values of Λ. It is clear from the figure that, with the increase of Λ, the loss peak shifts towards the shorter wavelengths and the related intensity increases. The reason behind this behavior is that, as the Λ increases, the light in the core penetrates more into the cladding, and the evanescent electromagnetic field increases which leads to loss enhancement.

It is well known that the performance of the RI plasmonic PCF sensor relies on the shift of the position of the resonance peak associated with the change of the detected analyte RI. Owing to the uniform distribution of the loss spectra and the single peak in the investigated band, the proposed sensor seems very proper for sensing applications. Fig. 7 displays the confinement loss spectra for different analyte RIs from 1.33 to 1.36. Using the wavelength–interrogation–method, when the RI varies from 1.33 to 1.36, the corresponding resonance wavelength can be tuned from 0.5 to 0.7 μm. Results reveals that the average $\Delta\lambda_{peak}$ is about

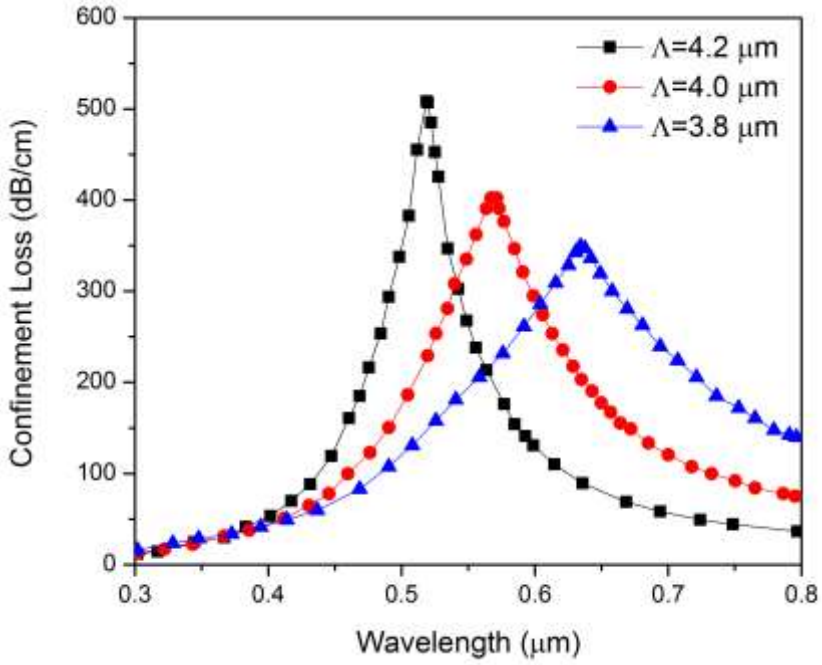

Fig. 6. Variation of the core mode confinement loss spectra of the proposed RI sensor for different values of the lattice pitch Λ.

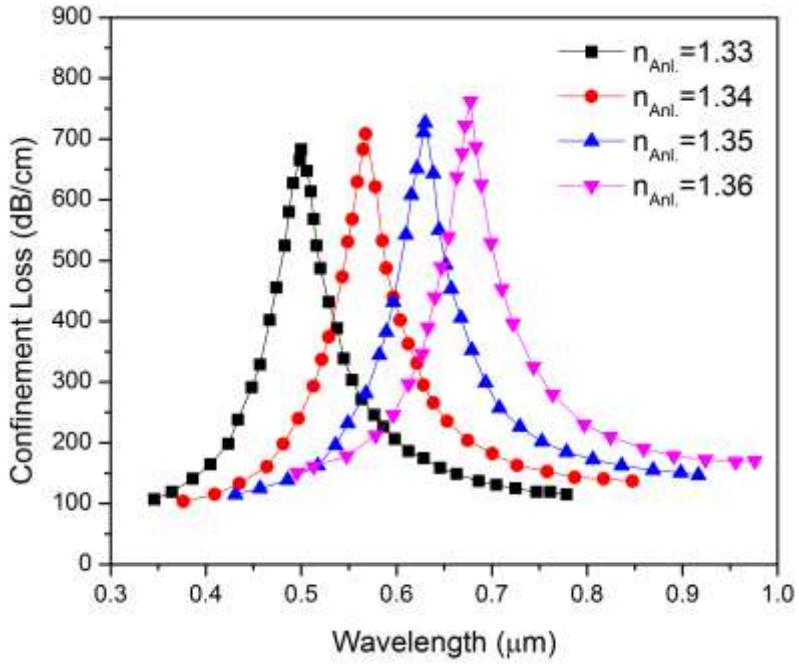

Fig. 7. Variation of the confinement loss spectra of the proposed RI sensor for different values of analyte RI.

77 nm; thus, the average wavelength sensitivity (S_n) (Eq. 4) is 7700 nm/RIU in this sensor. The maximum S_n occurs as the analyte RI varies from 1.33 to 1.34. The maximum sensitivity reaches 9500 nm/RIU, and the corresponding RI resolution is 6.5×10^{-6} RIU. Fig. 8 exhibits the amplitude sensitivity with different analyte RIs calculated by AIM. We observe that the corresponding peak intensity decreases as RI changes from 1.33 to 1.36, and maximum amplitude sensitivity reaches 215 RIU^{-1} when $n_{Anl.}$ is 1.33.

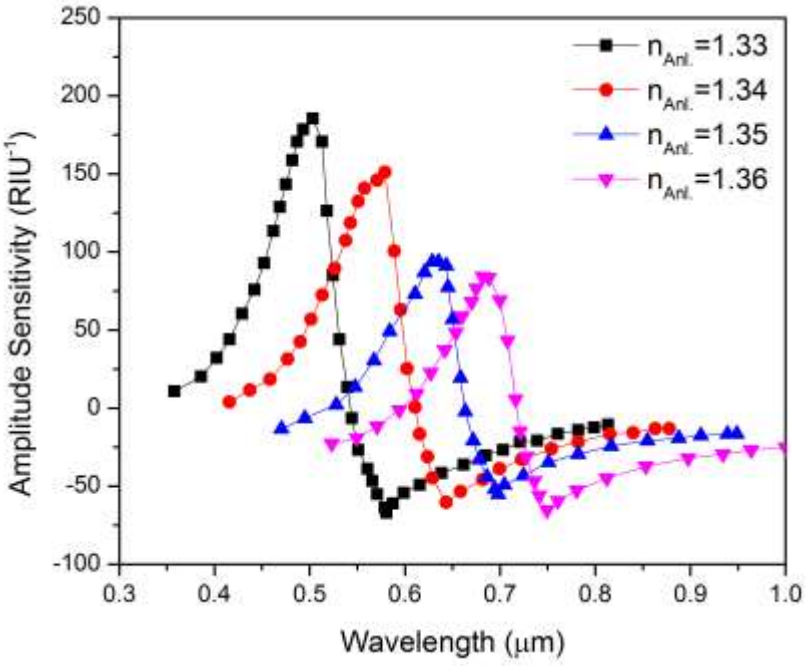

Fig. 8. The calculated amplitude sensitivity of the proposed sensor for different analyte Ris.

Finally, we analyzed the linearity of the proposed sensor by fitting the values of the resonance wavelengths versus analyte RIs (Fig. 9):

$$\lambda_{Peak} = 6.6 n_{Anl.} - 8.3 \qquad (6)$$

The adjusted residual–square (R^2) of 0.99862 was found for the fitting equation indicating a highly linear correlation degree between $n_{Anl.}$ and λ_{Peak}.

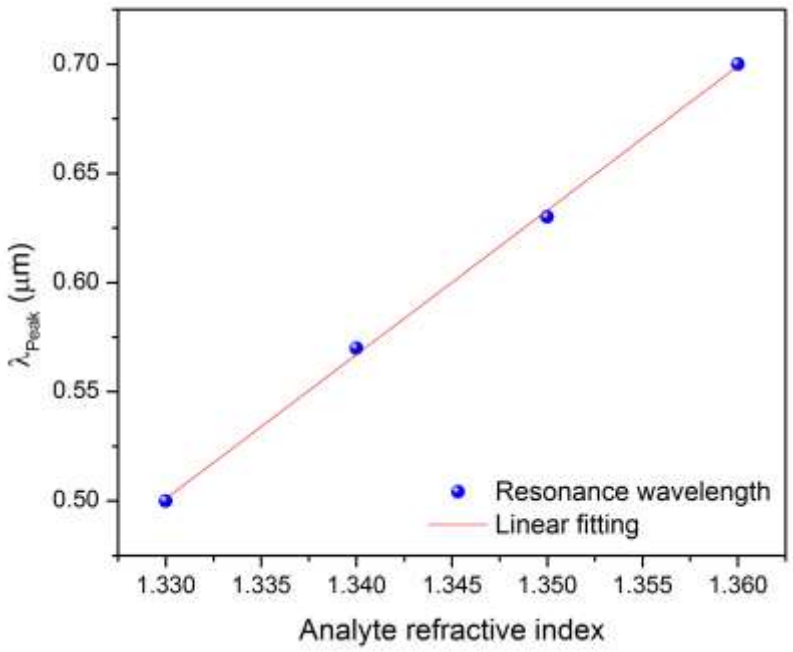

Fig. 9. The analysis of linearity degree between the resonance wavelength and analyte RI.

Compare to the other structures [10–12], the convenient design and high sensitivity of the proposed sensor, make it suitable for many applications.

4. Conclusion

In brief, we numerically analyzed the sensing properties of a high-performance visible D-shaped PCF–SPR RI sensor. The finite element method was used to investigate the sensing performance. The effect of the structural characteristics, and the relation between the resonance wavelengths and analyte refractive index were also studied. Using the wavelength interrogation method, an average wavelength sensitivity of 7700 nm/RIU and an average RI resolution of 1.08×10^{-5} RIU were attained. Also, the maximum wavelength sensitivity and RI resolution of 9500 nm/RIU and 6.5×10^{-6} RIU ware achieved, respectively, for the analyte RI between 1.33 and 1.34. Furthermore, the amplitude sensitivity of 215 RIU^{-1} at $n_{Anl.}$=1.33 was observed from the calculations.

Funding declaration

This study didn't use any fund.

Author declaration

[Instructions: Please check all applicable boxes and provide additional information as requested.]

1. Conflict of Interest

Potential conflict of interest exists:

We wish to draw the attention of the Editor to the following facts, which may be considered as potential conflicts of interest, and to significant financial contributions to this work:

The nature of potential conflict of interest is described below:

☒No conflict of interest exists.

We wish to confirm that there are no known conflicts of interest associated with this publication and there has been no significant financial support for this work that could have influenced its outcome.

2. Funding

☐Funding was received for this work.

All of the sources of funding for the work described in this publication are acknowledged below:

[List funding sources and their role in study design, data analysis, and result interpretation]

☒No funding was received for this work.

3. Intellectual Property

☒We confirm that we have given due consideration to the protection of intellectual property associated with this work and that there are no impediments to publication, including the timing of publication, with respect to intellectual property. In so doing we confirm that we have followed the regulations of our institutions concerning intellectual property.

4. Research Ethics

☒We further confirm that any aspect of the work covered in this manuscript that has involved human patients has been conducted with the ethical approval of all relevant bodies and that such approvals are acknowledged within the manuscript.

☒IRB approval was obtained (required for studies and series of 3 or more cases)

☒Written consent to publish potentially identifying information, such as details or the case and photographs, was obtained from the patient(s) or their legal guardian(s).

5. Authorship

The International Committee of Medical Journal Editors (ICMJE) recommends that authorship be based on the following four criteria:

1. Substantial contributions to the conception or design of the work; or the acquisition, analysis, or interpretation of data for the work; AND
2. Drafting the work or revising it critically for important intellectual content; AND
3. Final approval of the version to be published; AND
4. Agreement to be accountable for all aspects of the work in ensuring that questions related to the accuracy or integrity of any part of the work are appropriately investigated and resolved.

All those designated as authors should meet all four criteria for authorship, and all who meet the four criteria should be identified as authors. For more information on authorship, please see http://www.icmje.org/recommendations/browse/roles-and-responsibilities/defining-the-role-of-authors-and-contributors.html#two.

☒All listed authors meet the ICMJE criteria. We attest that all authors contributed significantly to the creation of this manuscript, each having fulfilled criteria as established by the ICMJE.

☐One or more listed authors do(es) not meet the ICMJE criteria.

We believe these individuals should be listed as authors because:

[Please elaborate below]

☒We confirm that the manuscript has been read and approved by all named authors.

☒We confirm that the order of authors listed in the manuscript has been approved by all named authors.

6. Contact with the Editorial Office

The Corresponding Author declared on the title page of the manuscript is:

Mojtaba Sadeghi

☒This author submitted this manuscript using his/her account in EVISE.

> ☒We understand that this Corresponding Author is the sole contact for the Editorial process (including EVISE and direct communications with the office). He/she is responsible for communicating with the other authors about progress, submissions of revisions and final approval of proofs.
>
> ☐We confirm that the email address shown below is accessible by the Corresponding Author, is the address to which Corresponding Author's EVISE account is linked, and has been configured to accept email from the editorial office of American Journal of Ophthalmology Case Reports:

☐Someone other than the Corresponding Author declared above submitted this manuscript from his/her account in EVISE:

[Insert name below]

> ☒We understand that this author is the sole contact for the Editorial process (including EVISE and direct communications with the office). He/she is responsible for communicating with the other authors, including the Corresponding Author, about progress, submissions of revisions and final approval of proofs.

Availability of data and material

All data are available whenever were asked.

Code availability

The code will be available whenever is asked.

Authors' contributions

1- Amin Sayyad Tondro performed the calculations.

2- Mojtaba Sadeghi analyzed the results and prepared the figures.

3- Abbas Kamaly contributed in writing the text.

4- Zahra Adelpour contributed in discussions.

5- Ali Emamghorashi contributed in analysis and discussion.

Ethics approval

I, Mojtaba Sadeghi, corresponding author of the manuscript, am enclosing herewith a manuscript entitled “Modeling and analysis of D-shaped plasmonic refractive index and temperature sensor using photonic crystal fiber” submitted to Journal of Computational Electronics for possible evaluation. With the submission of this manuscript I would like to undertake that the above mentioned manuscript has not been published elsewhere, accepted for publication elsewhere or under editorial review for publication elsewhere; and that my Institute’s Islamic Azad University, Shiraz branch representative is fully aware of this submission.

Submitted manuscript is an original research article.

Sincerely Yours,

Mojtaba Sadeghi, PhD

Consent to participate

Author Agreement Statement

We the undersigned declare that this manuscript is original, has not been published before and is not currently being considered for publication elsewhere. We confirm that the manuscript has been read and approved by all named authors and that there are no other persons who satisfied the criteria for authorship but are not listed. We further confirm that the order of authors listed in the manuscript has been approved by all of us. We understand that the Corresponding Author is the sole contact for the Editorial process. He is responsible for communicating with the other authors about progress, submissions of revisions and final approval of proofs Signed by all authors as follows:

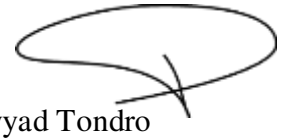

1- A. Sayyad Tondro

2- M. Sadeghi

3- A. Kamaly

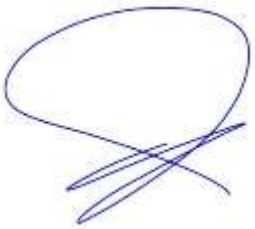

4- Z. Adelpour

5- A. Emamghorashi

Consent for publication

I, the undersigned, give my consent for the publication of identifiable details, which can include photographs and details within the text to be published in the above Journal and Article.

Dr. Mojtaba Sadeghi

Corresponding Author

References

[1] P. W. Russell, Photonic crystal fibers. Science 299 (2003) 358–362.

[2] P. Russell, Photonic Crystal Fibers. J. Lightwave Technol. 24 (2006) 4729–4749.

[3] M. Tian, P. Lu, L. Chen, C. Lv, D. Liu, All–solid D–shaped photonic fiber sensor based on surface plasmon resonance. Opt. Commun. 285 (2012) 1550–1554.

[4] R. K. Gangwar, V. K. Singh, Highly Sensitive Surface Plasmon Resonance Based D–Shaped Photonic Crystal Fiber Refractive Index Sensor. Plasmonics, 12 (2017) 1367–1372.

[5] J. Wu, S. Li, X. Wang, M. Shi, X. Feng, Y. Liu, Ultrahigh sensitivity refractive index sensor of a D–shaped PCF based on surface plasmon resonance. Appl. Opt. 57 (2018) 4002–4007.

[6] R. M. Osgood, N. C. Panoiu, J. I. Dadap, X. Liu, X. Chen, I. Hsieh, E. Dulkeith, W. M. J. Green, Y. A. Vlasov, Engineering nonlinearities in nanoscale optical systems: Physics and applications in dispersion–engineered silicon nanophotonic wires. Adv. Opt. Photonics, 1 (2009) 162–235.

[7] J. N. Dash, R. Jha, On the performance of graphene–based D–shaped photonic crystal fiber biosensor using surface plasmon resonance, Plasmonics, 10(5) (2015) 1123–1131.

[8] Y. Zhang, L. Xia, C. Zhou, X. Yu, H. Liu, D. Liu, Y. Zhang, Microstructured fiber based plasmonic index sensor with optimized accuracy and calibration relation in large dynamic range, Opt. Commun. 284 (2011) 4161–4166.

[9] G. An, S. Li, X. Yan, X. Zhang, Z. Yuan, H. Wang, Y. Zhang, X. Hao, Y. Shao, Z. Han, Extra–broad photonic crystal fiber refractive index sensor based on surface plasmon resonance, Plasmonics 12(2) (2017) 465–471.

[10] J. Wu, S. Li, X Wang, M. Shi, X. Feng, Y. Liu, Ultrahigh sensitivity refractive index sensor of a D–shaped PCF based on surface plasmon resonance. Appl. Opt. 57 (2018) 4002–4007.

[11] K. C. Ramya, K. V. Kumar, K. Geetha, C. S. Boopathi, Design of D shaped plasmon–photonic crystal fiber for bio sensing application. Results Phys. 10 (2018) 993–994.

[12] J. Lu, Y. Li, Y. Han, Y. Liu, J. Gao, D–shaped photonic crystal fiber plasmonic refractive index sensor based on gold grating. Appl. Opt. 57 (2018) 5268–5272.